

PORE-SCALE SIMULATION OF FLUID FLOW IN PACKED-BED REACTORS VIA RIGID-BODY SIMULATIONS AND CFD

*Original*

PORE-SCALE SIMULATION OF FLUID FLOW IN PACKED-BED REACTORS VIA RIGID-BODY SIMULATIONS AND CFD / Boccardo, Gianluca; Luigi DEL, Plato; Marchisio, Daniele; Frederic, Augier; Yacine, Haroun; Daniel, Ferre; Icardi, Matteo. - ELETTRONICO. - (2014). ( 10th International Conference on Computational Fluid Dynamics In the Oil & Gas, Metallurgical and Process Industries Trondheim June 17-19, 2014).

*Availability:*

This version is available at: 11583/2551737 since:

*Publisher:*

SINTEF/NTNU

*Published*

DOI:

*Terms of use:*

This article is made available under terms and conditions as specified in the corresponding bibliographic description in the repository

*Publisher copyright*

(Article begins on next page)

## PORE-SCALE SIMULATION OF FLUID FLOW IN PACKED-BED REACTORS VIA RIGID-BODY SIMULATIONS AND CFD

Gianluca BOCCARDO<sup>1\*</sup>, Luigi DEL PLATO<sup>1</sup>, Daniele MARCHISIO<sup>1</sup>, Frederic AUGIER<sup>2</sup>, Yacine HAROUN<sup>2</sup>, Daniel FERRE<sup>2</sup>, Matteo ICARDI<sup>3</sup>

<sup>1</sup>DISAT - Politecnico di Torino, Torino, ITALY

<sup>2</sup>IFP Energies nouvelles, Rond point de l'échangeur de Solaize, BP3, 69360 Solaize, France

<sup>3</sup>CEMSE - KAUST, Thuwal, Saudi Arabia

\* E-mail: gianluca.boccardo@polito.it

### ABSTRACT

The problem of fluid flow in porous media is of paramount importance in the process, oil and metallurgical industries, since it is involved in the extraction of minerals and oil, in aquifer dynamics, as well as chemical reactions carried out in fixed bed catalytic reactors. Its CFD simulation is particularly interesting, as it offers the possibility of reducing the extent of costly experimental investigations, but presents a number of technical challenges. One of the main issues is the generation of a geometrical model that realistically represents the porous medium/particle packing. Its derivation from experiments (i.e. micro-computer tomography) is complicated and packing codes are often limited to simple convex (mainly spherical) objects. In this work a computational tool developed in computer graphics, and integrated with the Bullet Physic Library, is used to generate realistic packings of polydisperse catalytic spheres and trilobes. The geometrical model is then meshed with SnapyHexMesh and then simulated with Ansys Fluent. Results show excellent agreement with experiments, demonstrating the great potentiality of the approach.

**Keywords:** Porous media, fixed bed catalytic reactor, Blender, Fluent, CFD, fluid dynamics, Ergun law.

### NOMENCLATURE

#### Greek Symbols

$\rho$	Mass density, [ $kg/m^3$ ]
$\mu$	Dynamic viscosity, [ $kg/ms$ ]
$\nu$	Kinematic viscosity, [ $m^2/s$ ]
$\varepsilon$	Porosity, [-]
$\varepsilon_m$	Geometric model porosity, [-]
$\varepsilon_g$	Meshed model porosity, [-]

#### Latin Symbols

$V_s$	Superficial velocity, [ $m/s$ ].
$P$	Pressure, [ $Kg/ms^2$ ].
$D_t$	Circumscribing trilobe diameter, [ $m$ ].
$D_g$	Grain diameter, [ $m$ ].
$D_g^*$	Effective grain diameter, [ $m$ ].
$L$	Domain length, [ $m$ ].

### INTRODUCTION

In chemical engineering many processes involve fixed bed (mainly catalytic) reactors and as such, the study of the hydrodynamics and transport phenomena inside these systems

are of great interest, and fundamental to their design. Usually, parameters of interest (such as mass transfer or dispersion coefficients) are obtained from the corresponding experimentally validated correlations, or from new experimental investigations. However, due to the geometrical features proper of these reactors, these studies are not at all straightforward: many small-scale complexities may arise, which have a great impact on the overall system behavior, both in the fluid flow and in transport processes. This makes the preparation of comprehensive bench-scale experiments difficult, and results in a challenging scale-up of the results obtained at the small-scale to the larger industrial scale of interest. Moreover, it is very difficult to explore the whole range of variation of the properties of interest, as for example the packed bed porosity, the size distribution of the catalyst particles and their shape. These issues are in fact shared by the larger field of study of flow and transport in random porous media. In this respect, an interesting alternative to experimental investigation is represented by computer simulations via computational fluid dynamics (CFD), which can help in limiting the number of experiments to be conducted and allowing for wider exploration of packing characteristics and operating conditions. Moreover, complex small-scale phenomena can be more deeply investigated, in a way usually not attainable with the use of experiments only. Many works have already demonstrated the effectiveness of this approach in the study of packed bed reactors (Augier *et al.*, 2010b,a).

In order to perform a reliable CFD simulation, the starting point is in the choice of an accurate geometric model representing the actual system, and it being as realistic as possible. Two ways of doing this are available. The first lies in using actual experimental data, be it via SEM imaging of the catalytic particles, micro-computer tomography scans of a portion of the packed bed loading, or other such methods. While these procedures have a merit in the precision with which the description of the medium at the pore-scale is obtained, they suffer from a great difficulty in the post-processing of these scans, in order to extract a suitable mesh for the CFD code, and in the high cost of the equipment needed for the experiment itself. The second possibility, and the one chosen in this work, is to rely on a *in-silico* algorithmic reconstruction of a geometrical model, which faithfully represents the real system in all of its features: the first advantage is the extremely lower cost of such an approach with respect to using the more sophisticated experimental techniques mentioned, coupled with the easiness of generating and testing a

very high number of loading realizations, with varying particle shapes and particle size distributions. Obviously, great care must be given as to ensure that the reconstructed model is accurate both as a purely geometrical description and, perhaps more importantly, in showing the same fluid dynamic behaviour of the real system under investigation.

The objective of this work is therefore to demonstrate the validity of the procedure just described, in both these aspects. First, a procedure for the replication of the catalyst loading process, via computer graphics and ballistic physics simulation, was developed and tested for a number of different catalyst shapes. A validation of the viability of the resulting geometries was performed, involving the comparison of the models void fractions with experimental results. In this way, a number of models representing different packed bed configurations were obtained. Also, a great deal of attention was given to the meshing process. Meshes with different levels of refinement were generated, and results concerning the evaluation of the critical cell size necessary to obtain both a good discretization of the grains surface and a precise description of the contact points between them, are shown. Finally, CFD simulations were performed on these systems: fluid flow was described by solving the continuity and Navier-Stokes equations. The results, especially regarding pressure drop in the bed, were compared to empirical models of pressure drop in porous media.

## THEORETICAL BACKGROUND

### Obtaining the geometric model

As mentioned, the first part of this work dealt with the development of a robust tool for effectively simulating the stacking of particles in a packed bed, with particular attention to catalytic particles and catalytic reactors. In order to do that the software `Blender` (Van Gumster, 2009) was used, which itself avails of the `Bullet Physics Library`, which is a large collection of codes used to manage the dynamics of rigid bodies and, most importantly, to detect and calculate the outcome of the collisions between these bodies. This library provides for a number of iterative methods combining accuracy, speed and robustness, enabling for the simulations of a very large number of elements, as it will be shown further on; moreover, a clear advantage of using this code with respect to many other algorithms used to recreate granular media models lies in the possibility to manage any particle shape, even complex non-convex ones, which are the ones of most difficult treatment in rigid body simulations. The choice of the code `Blender` was also made due to its extensive scripting functionality. A tool was then developed (in the language `Python3`) and plugged into the main rigid body simulation code, with the purpose of quickly setting up different simulation cases, with several particle shapes, particle size distributions, total numbers, and containers in which the particles settle. The shapes considered were spheres and trilobe extrudates, while the containers tested were cubes and cylinders. An example of two cylindrical loadings, one of spheres and one of trilobes, can be found in Fig. 1

Since the purpose is to mimic the loading of the catalyst beads into the reactor in a realistic manner, the particles are initially placed on top of the container, with gravity causing their deposition into it, with the end state of the simulation provided by a stable solution of the balance of the forces acting on them, namely gravity and the interaction forces. The choice of the initial placement of the grains in the setup of the rigid body simulation is a step worth mentioning. As mentioned, the purpose is to replicate the process of physically

filling the reactor with catalyst particles as accurately as possible: to that end, different ways of funneling the particles in the system have been devised and tested, and they are shown in Fig. 2.

In short, the first way is the simplest to implement but the less realistic one, with every particles falling in the container through a single straight line, while the other two represent the actual process quite well, with the random “grid” placement giving the best results. The difference in the latter lies in the additional step of allowing for a certain distance between the grids, resulting in more time for each set of particle to settle and thus in a more stable simulation. When items which do not possess spherical symmetry are considered, such as trilobes, a randomization is also added to their original orientation during their placement in the grid.

Two other very important points in the setup of the physical simulation concern the geometric description of the particles during the resolution of the collision events and the mechanical parameters governing their behavior. All particle shapes are represented in `Blender` with a “watertight” (closed) external mesh, constituted of triangular or quadrangular elements. Hence, the representation of a sphere (for example) will depend on the definition with which the surface is discretized: its refinement level. The higher this refinement level is, the better the model will be but also obviously the heavier the computational cost for calculating the rigid body dynamics and collision events will be. For example, a sphere with refinement level equal to 1 is an icosahedron, with each further refinement level splitting each triangular face into four triangles, resulting in a smoother surface. In the results section the choice for a suitable trade-off in this matter will be presented and justified. Moreover and even more importantly, a choice has to be made of the collision model of the particle. Many times in fact it may not be necessary to use an object surface mesh: in the simple case of a sphere for example, only a two-parameter description (its center and its radius) is necessary to perfectly describe its position and behavior in the physical simulation. The savings in both memory requirements and computational cost with respect to the use of the full surface mesh is evident. There are of course scales of increasing complexity: for an highly non-spherical convex

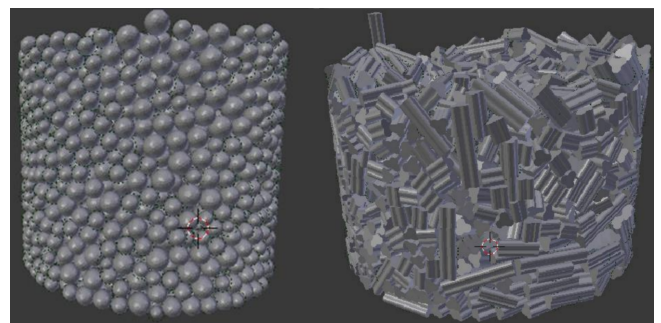


Figure 1: Packing of spheres and trilobes in cylindrical containers.

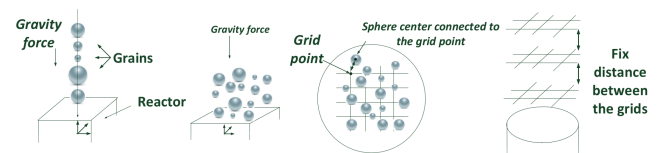


Figure 2: Three different types of initial particle placement.

shape the computation of the nearest-approximating convex hull will be needed, and the most complex case is that of a non-convex shape, and the trilobes considered in this work pertain to this category. In this last case, the whole surface mesh will be needed during the rigid body dynamics computation, leading in a more expensive simulation with respect to the case of spheres.

Lastly, the parameters governing the calculation of interactions between the objects have to be considered: these are the friction factor and the coefficient of restitution. Both of these parameters can be modified, greatly influencing the outcome of the physical simulation. In almost all cases, these settings have been specified in order to replicate the real physical characteristics of the materials involved, but in some cases this was not the most desirable course of action. For the case of trilobes, using the true values for these parameters led to an unrealistic geometric model, showing an excessive packing anisotropy and porosity. In this case, these two parameters were then tuned (reducing the friction factor and increasing the restitution coefficient) in order for the geometrical characteristics of the resulting model to match corresponding validated experimental data. The rationale in this case was to give priority to obtain a realistic and precise simulation result over trying to describe accurately the intermediate deposition and settling steps: the same methodology was followed in (Augier *et al.*, 2010b), where a DEM (Discrete Elements Method) approach was used, in order to improve the density of the loading. Results pertaining this effect and our solution for it will be presented in the next section.

## Mesh Generation

After having obtained the geometric models with Blender and having validated them, the analysis of the pressure drop through the identified granular beds was conducted. In this work, fluid flow results pertaining to two different geometric models will be presented. The first one is a rectangular cuboid sample of a packing of Gaussian distributed spheres with average diameter equal to 1.99 mm and standard deviation equal to 0.29, with square faces 9 mm in size and 24 mm long in the direction parallel to fluid flow. The second model share the same bounding volume of the first one but the packing is constituted by trilobes, with circumscribing diameter  $D_t = 1.8$  mm (and equivalent diameter  $D_g = 1.44$  mm), with a Gaussian distribution in length with average length equal to 4.77 mm and standard deviation equal to 1.8.

A mesh was thus created for these two cases, to be used in the finite volume CFD code. The mesh utility `snappyHexMesh`, included in the open-source package `OpenFOAM` (OpenCFD, 2013), was used. The first step in the meshing process is the creation of a structured, cartesian grid in the entirety of the bounding volume of the system considered. Next, the volume pertaining to the geometric model is subtracted, leaving a cartesian grid in the fluid portion approximating the particles surface with a stair-step description. Finally, the mesh is further modified by moving each boundary vertex, relocating them closer to the original model surface, resulting in a body fitted mesh. The mesh generation process is critical to both obtaining grid independent results during the fluid flow simulation, and for ensuring that the CFD model constitutes a faithful representation of the original geometry. In all the simulations presented in this work, the cell layer next to the surface of the particles underwent an additional refinement step, to account for the sharper momentum boundary layer near the walls and thus adequately describing it. Moreover, a certain level of refine-

ment near the surface of the particles is necessary to give a satisfactory definition of the contact points, which can be wrongly approximated as larger contact solid volumes if too coarse a mesh is employed. An example of this phenomenon is given in Fig. 3.

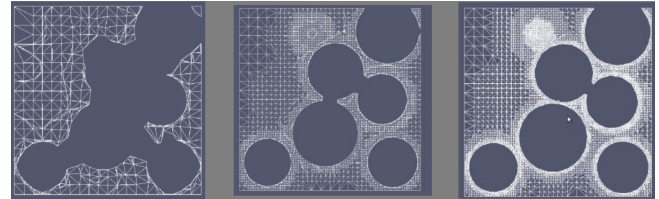


Figure 3: Grain surface definition at three increasing mesh refinement levels.

Moreover, the mesh porosity strictly depends on the dimension of the cells around the grains: an adequate number of cells is needed for the discretized model in the mesh to adequately represent the original model. Again, Fig. 3 visually clarifies this phenomenon. In order to quantify the number of cells needed in a mesh a study was conducted, by analyzing a 7 mm sized sample in a larger packing, constituted of a Gaussian distribution of spheres of average diameter equal to 1.99 mm. The porosity of the actual model, result of the Blender simulation, is 0.344. Then, several meshes with different cell dimensions were created, and the ratio between the porosity of the meshed sample and the original geometry,  $\epsilon_m/\epsilon_g$ , is calculated. The results are presented in Fig. 4.

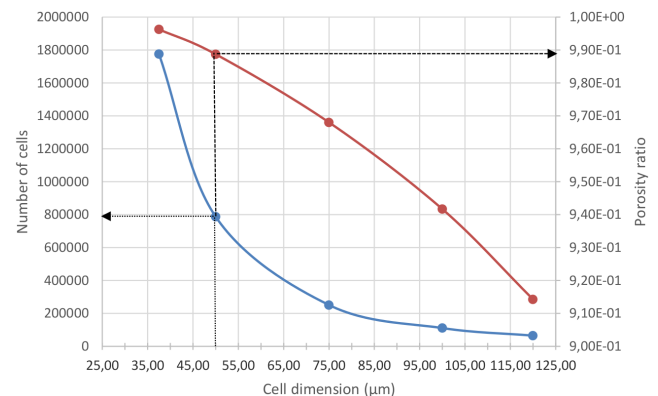


Figure 4: Porosity ratio and number of cells versus cell dimension for a spheres packing

As it can be seen, very coarse meshes can result in a very low  $\epsilon_m/\epsilon_g$  ratio, down to  $\epsilon_m/\epsilon_g = 0.9$ , while a grid with mesh cell size of  $50 \mu m$  (corresponding to 800,000 cells in this sample geometry) led to  $\epsilon_m/\epsilon_g = 0.989$ , which corresponds to a faithful representation of the original model. The acceptable cell dimension obviously depends on the average particle diameter: this result shows that an analysis of this type is a necessary step during the mesh generation process.

Finally, a further modification has been made to the final meshes, in which premixing and postmixing zones were added to the mesh (of size equal to approximately 2 grain diameters), respectively before the inlet and after the outlet. This was done with the purpose of obtaining a well developed velocity profile at the surface bordering the granular volume, and reduce flow anomalies (backflow, recirculation) due to the complex nature of the packing. This procedure was already employed in another work studying pore-scale flow in complex geometries, with good results (Boccardo *et al.*,

2014): the result of this operation and the final mesh can be seen in Fig. 5 and Fig. 6. The final meshes for the spheres and the trilobe packing are approximately of the same size, with around 5 million cells, with cells  $50 \mu\text{m}$  in size next to the grains surface and  $100 \mu\text{m}$  in size in the fluid bulk. The first packing contains about 200 spheres, with a resulting porosity of 0.355, while the other one contains about 100 trilobes, with a resulting porosity of 0.388.

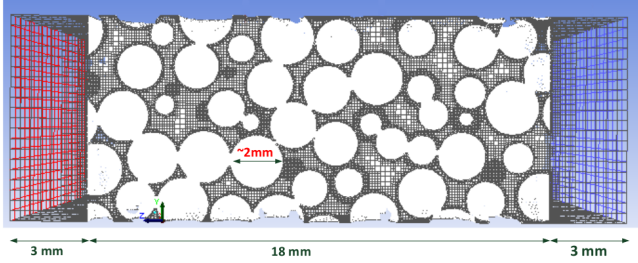


Figure 5: Final mesh, packing of spheres

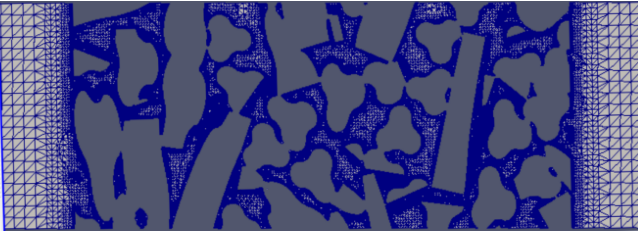


Figure 6: Final mesh, packing of trilobes

## Pore-scale CFD simulations

Using the meshes obtained as described in the previous part, fluid dynamic simulations are performed using the CFD code Ansys Fluent 15. The fluid velocity field was determined by solving the continuity and Navier-Stokes equations. A no-slip boundary condition was applied on the grain surface. An inlet zone was set on one side of the geometry (one of the two smallest faces of the rectangular cuboid), with fluid entering the domain at a fixed velocity, and an outlet zone at the opposite face, with a condition of zero relative pressure. No additional forces (like gravity), were considered. On the remaining sides a condition of symmetry was set, implying no fluid flow across these surfaces. The fluid considered was air, with density  $\rho = 1.225 \text{ kg m}^{-3}$  and dynamic viscosity  $\mu = 1.789 \times 10^{-5} \text{ kg m}^{-1}\text{s}^{-1}$ . The range of superficial velocities,  $V_s$ , explored went from  $0.01$  to  $0.1 \text{ m s}^{-1}$  ( $0.3 < \text{Re} < 30$ ). The system was solved for in laminar conditions and under steady-state, with density and viscosity considered constant. The energy equation was not solved.

The most important result of these simulations was the calculation of pressure drop, which was simply calculated as the difference between values of static pressure at the start and at the end of the actual granular bed. To clarify: the pressure drop was calculated in the inner zone where the packing was present, ignoring the conditions in the outer pre- and post-mixing “buffer” zones.

These results were then compared with the predictions from Ergun law, usually employed to describe flow in packed filter beds:

$$\frac{\Delta P \rho D_g}{G_0^2 L} \frac{\varepsilon^3}{(1 - \varepsilon^3)} = 150 \frac{1 - \varepsilon}{(D_g G_0) / \mu} + 1.75, \quad (1)$$

where  $G_0$  is the mass flux ( $G_0 = \rho V_s$ )  $\varepsilon$  is the porosity.  $D_g$  is the grain size: in the case of spheres it is the corresponding Sauter diameter, while for the trilobes it is the calculated equivalent diameter. This value is obtained following the findings of (Boyer *et al.*, 2007), where the empirical correlation  $D_g = C D_t$  was found to provide the best agreement between the experimental data and Ergun law. The empirical factor  $C$  depends on the trilobe size, and is equal to 0.8 in this case.

Grid independence of the CFD results also needed to be ensured: the parameter used to assess this is the equivalent diameter  $D_g^*$ . Following a methodology used and described in greater detail in a previous work (Boccardo *et al.*, 2014), each different mesh refinement level is characterized by an effective diameter  $D_g^*$ , which is used as a fitting parameter comparing the pressure drop results from steady-state flow simulations at different fluid velocities to the predictions of the Ergun law for that operating conditions. Variations of  $D_g^*$  versus cell dimension can then be analyzed, and the mesh ensuring grid independent result identified. Results for the case of a packing of Gaussian distributed spheres with an average diameter of  $2 \text{ mm}$  can be found in Fig. 7. In this case, a cell dimension of  $50 \mu\text{m}$  will result in a satisfactory discretization of the momentum boundary layer.

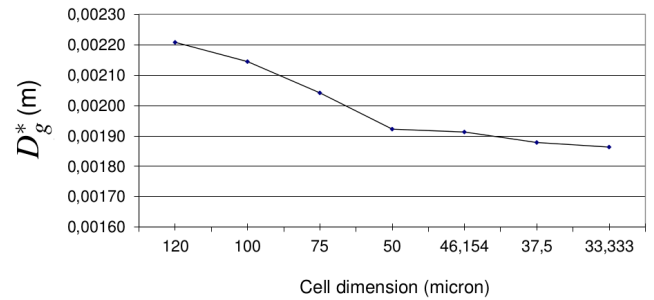


Figure 7: Effective grain size,  $D_g^*$ , with varying cell dimension

## RESULTS

### Geometrical Models Validation

The first test done had the purpose of identifying a suitable “size” of the simulation (regarding the total number of grains), in order to identify the smallest representative elementary volume (REV) for the system under investigation. A cubic container,  $2.3 \text{ cm}$  in size, was filled with 1772 spherical particles, distributed along a Gaussian distribution with an average diameter of  $1.99 \text{ cm}$ . Cubic samples of different dimensions were taken inside the system, all centered in the center of gravity of the domain, and the corresponding porosity was computed: the results are shown in Fig. 8. Three different packings, with spheres of different refinement level, are analyzed.

At smaller dimensions, very high porosities are reported: this is expected as for sample sizes of the order of the grains diameter a disproportionately high fraction of a pore or a grain could end up in the sample. At  $5 \text{ mm}$  and for bigger sizes, the reported porosities reach a stationary value around 0.355, showing another instability arising only with sample sizes of the order of the container size, where wall effects come into

play (Zou, 1995). Finding this behavior for this kind of analysis is very satisfactory and equivalent results can be found in other examples in the literature (Bear, 1988). Moreover, this offers an indication for the choice of a refinement level for the particles description: as it can be seen, there are not substantial differences between the three cases except for small sample sizes. What is indicated as refinement level 3 is the most suitable for these applications, as it combines a good representation of the actual shape with an acceptable computational cost during the packing simulation.

Cylindrical containers were also tested, as they resemble the actual reactor shape; moreover, lab-scale experiments are also usually carried out in cylindrical test containers. A poly-disperse Gaussian distribution of 4000 particles, with an average diameter equal to 1.99 mm, is loaded with the random grid technique in a series of different containers, as specified in Tab. 1. As expected, since the same particle distribution is used in all cases, the results are very close at around  $\epsilon = 0.36$ ; this result is also in line with data (pertaining to the same particle size) coming from a large experimental campaign dealing with the study of flow conditions in trickle bed reactions (Boyer *et al.*, 2007).

Case	Container		Samples		$\epsilon$ (-)
	Diameter (cm)	Height (cm)	Diameter (cm)	Height (cm)	
P1	3	3	2.9	2.9	0.362
P2	3.5	3	3.35	2.27	0.358
P3	3.7	2.8	3.5	2.2	0.359
P4	4	2.4	3.9	2	0.359

Table 1: Porosity for spherical particle loadings in four different containers, with the corresponding sample dimensions.

For each geometry the porosity has been calculated both via averaging a series of 50 cylindrical samples randomly placed in the container (with diameter and height both equal to 5 mm), and via calculating the global packing porosity: the latter is reported in Tab. 1. It has to be noted that the dimension of the global sample is slightly lower than that of the container itself: again, this is a necessary precaution in order to avoid the effect of the presence of the walls on this sampling operation, which would markedly affect the porosity reported, with increases of up to one percent.

This wall effect has also been more deeply investigated by examining the packing P3 (as referred to in Tab. 1). In this case a different sampling strategy has been adopted: 200 annular samples, with height equal to 2 cm, were taken. Each of these was placed at the center of the container, and each had

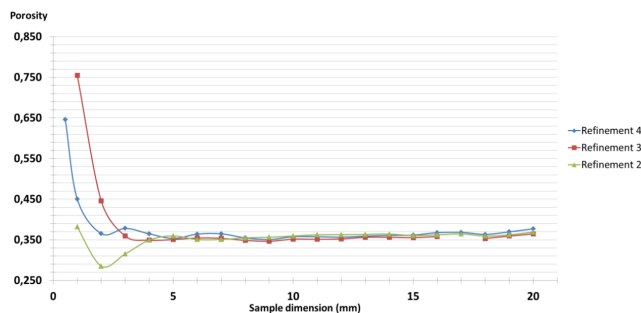


Figure 8: Porosity for increasingly large cubic samples, for three different spheres refinement levels

a fixed volume but an increasing diameter, effectively calculating the local porosity value along the radial direction from the center of the packing. The results are shown in Fig. 9

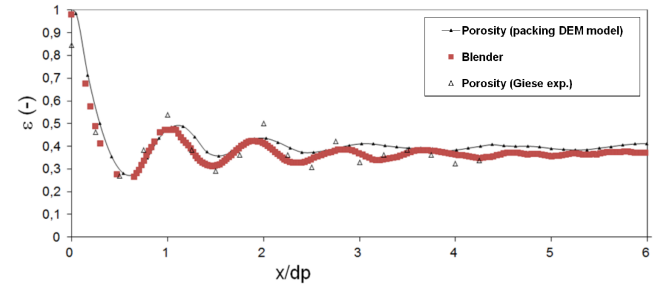


Figure 9: Comparison of local porosity values: old packing model (black symbols), current work packing model (red symbols) and experimental data (white triangles).

In the same figure, these results are compared with two other analyses of the same type: one conducted on an earlier study of an algorithmically generated packing (Augier *et al.*, 2010b), and the other one being actual experimental data (Giese *et al.*, 1998). The accordance between the results obtained in this work and the experimental data is satisfactory, as it confirms that the physical simulation replicates the characteristics of a real packing consistently.

Lastly, tests were conducted with trilobe packings in cylindrical containers: a Gaussian distribution in length of 3000 trilobes with an average length of 4.77 mm and a circumscribing diameter  $D_t = 1.8$  mm (and equivalent diameter  $D_g = 1.44$  mm) and standard deviation equal to 1.8 was considered, in a container with diameter and height respectively equal to 3.5 cm and 3 cm.

As mentioned before, the setup of the physical simulation in the case of the trilobe shape is of the utmost importance, as the resulting loading porosity will vary widely depending on the choice of the bounding volume and of the particular friction factor and coefficient of restitution used. Three simulations comparing different settings of these two parameters were performed, and both the global bed porosity and the porosity distribution inside the bed (using a number of randomly placed samples) were calculated. The results are shown in Tab. 2.

Cases	Restitution coefficient	Friction factor	Total $\epsilon$ (-)	Sampled $\epsilon$ (-)
T1	0	0.5	0.415	0.411
T2	0.7	0.325	0.39	0.377
T3	0.85	0.325	0.378	0.364

Table 2: Restitution coefficient and friction factor used in three different packing simulations of trilobes, with the resulting total and sampled porosity.

The data shown in this table show how strongly these two physical parameters influence the mixing effect mentioned earlier, and hence the resulting bed porosity. Once again it has to be noted that the total bed porosity is higher than the average porosity calculated through sample averaging, due to the presence of the walls. The difficulties in treating the dynamics of rigid body interactions in the case of such a complex particle shape notwithstanding, it stands to notice that when the right set of collision parameters is used (cases T2 and T3) a remarkable accordance to experimental data was found (Boyer *et al.*, 2007).

## Fluid Flow Results

### Packing of spheres

The first interesting result can be found in Fig. 10, where the pressure profile (for  $Re = 3.47$ ) for the first geometry (packing of spheres) is shown in comparison with the predictions of Ergun law. The fact that the system shows a linear pressure profile is a good indicator of the validity of the simulated sample chosen, and that can be considered a representative

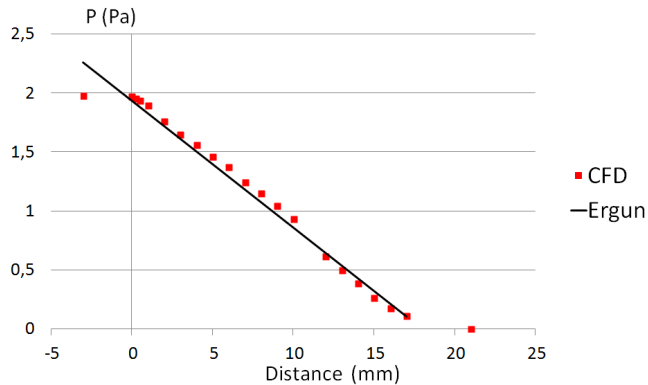


Figure 10: Pressure profile inside the granular medium for the packing of spheres,  $Re = 3.47$

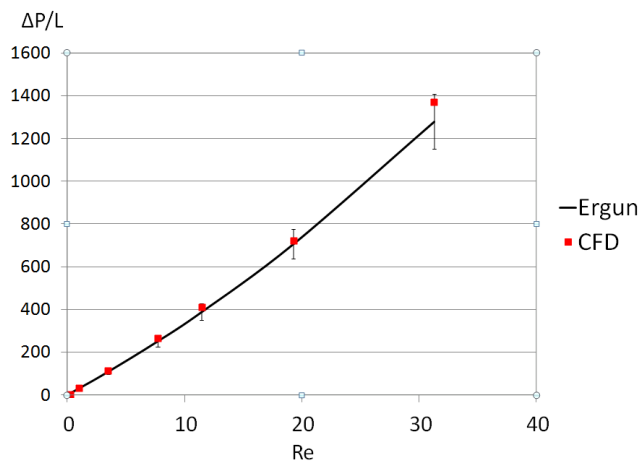


Figure 11: Pressure drop versus  $Re$ , CFD results (red squares) and Ergun law predictions (continuous line) for the packing of spheres

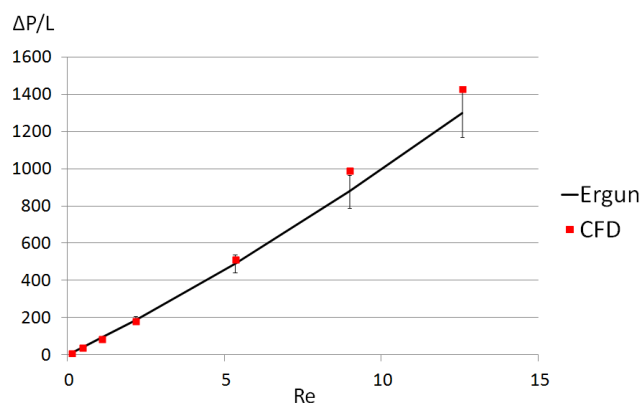


Figure 12: Pressure drop versus  $Re$ , CFD results (red squares) and Ergun law predictions (continuous line) for the packing of trilobes

volume for the granular system investigated in this case. The first and last points in the graph, apparent outliers, refer to points in the fluid buffer zone, and are not thus considered.

The aggregate results for all the superficial velocities considered can be found in Fig. 11, again compared to Ergun law. As it is shown, the CFD results follow the predictions of the theoretical law within a 10% error margin, as evidenced by the error bars.

### Packing of trilobes

The same results were obtained for the other geometric model, the packing of trilobes. Again, the pressure profile along the granular medium was linear, exhibiting the same behavior shown in Fig. 10. Moreover, Fig. 12 shows that even for this complex catalyst shape, the results of the CFD simulations matched the predictions of Ergun law to a good degree, again showing a disparity less than 10% in value. It is worth mentioning here that the mean grain size used in the Ergun law, reported in Eq. (1), was derived in a previous internal study carried out at IFP Energies nouvelles, based on a very large number of experiments. Therefore the agreement between CFD simulations and the Ergun law in this context should be considered as an equivalent validation with experiments.

## CONCLUSION

In this work a computational tool developed in computer graphics, `Blender`, integrated with the `Bullet Physics Library`, is used to generate realistic packings of (catalyst) particles of different shapes. The main advantage of this approach (versus other alternatives) stands in the possibility of simulating packings constituted by particles with complex shapes (e.g. non-convex objects such as trilobes).

Results show that attention should be paid to the strategy with which particles are inserted into the container, as well as to the meshing procedure, carried out here with `snappyHexMesh`. The mesh has to be fine enough to describe well the geometrical details of the pores within the packing, as well as the momentum boundary layer around each particle. The validation with experimental data demonstrate that the generated packings realistically describe the behaviour of catalytic fixed bed reactors. In particular, when working with polydisperse spherical particles, the well known radial porosity profiles are obtained, with an accuracy superior to other similar tools. Moreover, pressure drop simulations, carried out with `Ansys Fluent` showed very good agreement with the predictions of the Ergun law (considered “exact” in this context). When working with polydisperse trilobes very good results are also obtained, especially considering that these complex non-convex objects are very difficult to treat. Also in this case comparison between simulated pressure drops and those predicted with the Ergun law (by using a grain size in turn obtained from corresponding experiments) showed excellent agreement. These results show that the approach developed in this work can be used to more deeply study the effect that the shape, size and length distribution of catalyst particles have on the fluid flow in fixed bed reactors, and improve existing models for pressure drop predictions.

In the next steps of our work chemical reactions and heat transfer will also be considered.

## Acknowledgments

The authors would like to acknowledge the help and useful suggestions of Rajandrea Sethi and Tiziana Tosco.

## REFERENCES

AUGIER, F. *et al.* (2010a). “Numerical approach to predict wetting and catalyst efficiencies inside trickle bed reactors”. *Chemical Engineering Science*, **65(1)**, 255 – 260. 20th International Symposium in Chemical Reaction Engineering-Green Chemical Reaction Engineering for a Sustainable Future.

AUGIER, F. *et al.* (2010b). “Numerical simulations of transfer and transport properties inside packed beds of spherical particles”. *Chemical Engineering Science*, **65(3)**, 1055 – 1064.

BEAR, J. (1988). *Dynamics of fluids in porous media*. Dover.

BOCCARDO, G. *et al.* (2014). “Microscale simulation of particle deposition in porous media”. *Journal of Colloid and Interface Science*, **417**, 227–237.

BOYER, C. *et al.* (2007). “Hydrodynamics of trickle bed reactors at high pressure: Two-phase flow model for pressure drop and liquid holdup, formulation and experimental validation”. *Chemical Engineering Science*, **62(24)**, 7026 – 7032. 8th International Conference on Gas-Liquid and Gas-Liquid-Solid Reactor Engineering.

GIESE, M. *et al.* (1998). “Measured and modeled superficial flow profiles in packed beds with liquid flow”. *AIChE Journal*, **44(2)**, 484–490.

OPENCDF (2013). *The Open Source CFD Toolbox, User Guide*. OpenCFD (ESI).

VAN GUMSTER, J. (2009). *Blender For Dummies*. Wiley.

ZOU, R. (1995). “The packing of spheres in a cylindrical container: the thickness effect”. *Chemical Engineering Science*, **50(9)**, 1504–1507.